Non-Hermitian Weyl fermions of types III and IV: Hamiltonian, topological protection, and Landau levels

Zaur Z. Alisultanov [1,2] and Edvin G. Idrisov [3]

[1]*ACTP, Moscow Institute of Physics and Technology, Dolgoprudnyi, Moscow Region 141701, Russia*

[2]*Institute of Physics of DFRS, Russian Academy of Sciences, Makhachkala 367015, Russia*

[3]*Department of Physics and Materials Science, University of Luxembourg, Luxembourg*

(Received 10 November 2021; revised 9 February 2023; accepted 13 February 2023; published 21 February 2023)

We adopt the non-Hermitian Hamiltonian formalism to describe Weyl fermions of types III and IV. The spectrum of Hamiltonian has an unusual type of anisotropy. Namely, the hermiticity of Hamiltonian strongly depends on the direction in momentum space: for some directions, the spectrum is real, in contrast for other directions it becomes complex. It is shown that the type III and IV Weyl points are topologically stable and the Chern number is equal to ± 1 despite to the fact that the Hamiltonian is not Hermitian. Furthermore, we calculate the Landau levels and demonstrate that zero Landau level is real, which means that there is a real spectral flow between electronlike and holelike states. Due to the formal analogy with the index theorem, the presence of such a flow as well indicates a nonzero Chern number. In addition, we illustrate that the non-Hermitian Hamiltonian can be regarded as a one-particle problem in the context of topological band theory.

DOI: 10.1103/PhysRevB.107.085135

I. INTRODUCTION

The current theoretical progress in band theory allows to describe topologically protected quasiparticles in modern experimentally accessible materials [1]. Due to their unique properties, for instance, chiral transport, the topological materials are expected to be promising for future electronics [2]. Among all, the topological materials with Dirac [3–6] and Weyl [7–11] points, as well as degenerate points [12] and lines [13–15] in the Brillouin zone are of particular interest. The massless fermions in such materials are topologically protected, which results in quantum-electrodynamics effects known from high-energy physics [16].

The idea of realization of Weyl points in condensed matter physics belongs back to C. Herring [17,18]. According to Herring's description, the presence of Weyl points can be understood within a two-band model. The corresponding Hamiltonian of in momentum representation can be presented in the Pauli basis

$$H(\mathbf{p}) = \sigma_0 f_0(\mathbf{p}) + \sum_{i=1}^{3} \sigma_i f_i(\mathbf{p}), \tag{1}$$

where σ_0 is 2×2 unit matrix, σ_i are Pauli matrices, and $\mathbf{p}$ is a three-dimensional (3D) momentum vector. The Weyl point $\mathbf{p}_\mathrm{W}$ arises due to crossing of bands, which satisfies to three algebraic equations $f_i(\mathbf{p}_\mathrm{W}) = 0$. Materials with these conditions are known as Dirac and Weyl semimetals [19]. Typically such kind of situation is easily realizable in 3D systems, and equations $f_i(\mathbf{p}_\mathrm{W}) = 0$ represent the two-dimensional (2D) surfaces in momentum space: three closed 2D surfaces can have many crossing points. In 2D systems, this condition corresponds to the crossing of three lines. This is not trivial and in order to have the Weyl point in 2D system, the certain types of symmetries (for example, C_{6v} point symmetry) are required [19]. In the vicinity of Weyl point $\mathbf{p}_W$, one can expand the function $f_i(\mathbf{p})$ in the Taylor series, which results in low-energy linear spectrum, namely, $f_i(\mathbf{p}) \propto |\mathbf{p}|$, and corresponding excitations are known as massless (Weyl or Dirac) fermions [19]. Equation (1) describes conventional (nontilted) type I Weyl fermions for zero and constant values of $f_0(\mathbf{p})$.

Apart from Weyl semimetals of type I, it was proposed Weyl semimetals of type II [20–23]. Nowadays such a kind of materials are accessible experimentally and WTe_2 is one of the candidates for a realization of type II Weyl fermions [24]. In short, the Hamiltonian for such systems can be modeled at the intersections of Fermi pockets and the spectrum turns out to be tilted. The minimal Hamiltonian for this case has the following form:

$$H(\mathbf{p}) = v_F \boldsymbol{\sigma} \cdot \mathbf{p} + \sigma_0 \boldsymbol{\omega} \cdot \mathbf{p}, \tag{2}$$

where v_F is Fermi velocity and $\boldsymbol{\omega}$ is a tilt vector. For $v_F > \omega$, this Hamiltonian describes the Weyl semimetals of type I with the tilted spectrum, and consequently, for $v_F < \omega$, the Hamiltonian corresponds to type II Weyl semimetals, where $\omega = |\boldsymbol{\omega}|$ is a modulus of vector. It is worth mentioning that Weyl semimetals of type II can be used for "modeling" of black and white holes, event horizons [25,26]. Indeed, assuming that the parameter of tilting, $\boldsymbol{\omega}(\mathbf{x})$, is a function of spatial coordinates, the Weyl fermions of type II can be described by an action of the massless spinor field [25]

$$\mathcal{S}_{II} = \int d^4x [i\overline{\psi}(v_F \gamma^\mu \partial_\mu + \gamma^0 \boldsymbol{\omega}(\mathbf{x}) \cdot \boldsymbol{\partial})\psi], \tag{3}$$

where ψ is a Dirac spinor and γ^μ is the Dirac matrix in the Weyl representation $\gamma^\mu = \left(\begin{smallmatrix} 0 & \sigma^\mu \\ \bar{\sigma}^\mu & 0 \end{smallmatrix}\right)$ with $\sigma^\mu = (\sigma_0, \boldsymbol{\sigma})$ and

$\tilde{\sigma}^\mu = (\sigma_0, -\boldsymbol{\sigma})$ and $\partial_\mu = (v_F^{-1}\partial_t, \boldsymbol{\partial})$. This is the possible basic (minimalistic) action for the description of massless spinor field in curved space with metrics $ds^2 = (|\boldsymbol{\omega}|^2 - 1)dt^2 - 2\boldsymbol{\omega}\cdot d\mathbf{x}dt + d\mathbf{x}\cdot d\mathbf{x}$ and allows to model phenomena in the vicinity of the event horizon.

In this paper, we make a further step to develop the theory for Weyl fermions of types III and IV. We show that these fermions can be described using the Hamiltonian formalism in the framework of non-Hermitian quantum theory. Moreover, the non-Hermitian Hamiltonian arises as a one-particle problem in the context of a band theory of Weyl semimetals. In order to study the properties of this Hamiltonian and associated Hilbert space, the acceptable theory of non-Hermitian systems is presented below. The spectrum of the Weyl Hamiltonian under consideration turns out to be anisotropic in momentum space, namely, for some directions, the spectrum is real, and for other directions, it is a complex quantity. The necessary and sufficient conditions for the real spectrum of the general Hamiltonian under consideration are formulated. The main feature of the system we are interested in is that the Chern number is equal to ± 1 despite to the non-Hermitian Hamiltonian and the zero Landau level is purely real. The existence of the real zero Landau level additionally confirms the nonzero Chern number. This is the direct consequence of analogy with the index theorem (see Ref. [37]).

The rest of the paper is organized as follows. In Sec. II, using the ideas of Refs. [27,28] we introduce the theory of Weyl fermions of types III and IV in Hamiltonian formalism and calculate the energy spectrum. In Sec. III, we provide the study the topological protection and associated Chern number. Section IV is devoted to the investigation of Landau levels and spectral flow. We present our discussion in Sec. V and conclusion in Sec. VI. Details of calculations are given in Appendices.

II. WEYL FERMIONS OF TYPE III AND IV

In recent seminal papers, Refs. [27,28], the authors have suggested Weyl fermions of types III and IV. Briefly, using the tetrad formalism, there was provided the general action of a massless spinor field of the form

$$\mathcal{S} = \int d^4x\sqrt{-g}\left[i\overline{\psi}\gamma^\nu e^\mu_\nu \partial_\mu \psi\right], \tag{4}$$

where g is the determinant of the metric tensor and e^μ_ν is the tetrad tensor. One can see from Eq. (4), that Weyl fermions of types I and II are particular cases of the general tetrad action theory. Indeed, if one keeps only diagonal elements of tetrad tensor $e^\mu_\nu = v_F\delta^\mu_\nu$, then we get the action for Weyl femions of type I. If one set $e^\mu_\nu = v_F\delta^\mu_\nu + \delta^0_\nu\omega^i\delta^\mu_i$, then we get the action for type II Weyl fermions presented in Eq. (3). However, in more general case, Eq. (4) can contain other nonzero components of the tetrad tensor, namely, $e^\mu_\nu = v_F\delta^\mu_\nu + \delta^0_\nu\omega^i\delta^\mu_i + \vartheta_i\delta^i_\nu\delta^\mu_0$, where ϑ_i are the components of additional tilt parameter vector $\boldsymbol{\vartheta}$. The presence of last term restores the symmetry with respect to rearrangement of indices μ and ν. Note that this form corresponds to a spatially isotropic tetrad when there is no $\delta^i_\nu\delta^\mu_j$ term. According to Ref. [27], the case $v_F > \omega$ and $v_F < \vartheta$ corresponds to Weyl fermions of type III, and $v_F < \omega$ and $v_F < \vartheta$ is associated with type IV, where $\vartheta = |\boldsymbol{\vartheta}|$. Due to the last term, $\vartheta_i\delta^i_\nu\delta^\mu_0$, the Lagrangian contains a new term with zero component of momentum $\sigma^i\vartheta_i p_0$ and $p_\mu = (p_0, p_i)$ with $p_0 = \varepsilon/v_F$. Particularly, the possible origin of this term and consequently Weyl points of types III and IV were associated with many-particle effects and thus can be worked out from the self-energy [27]. It is worth mentioning that in the framework of Hermitian quantum mechanics, the Hamilton formalism does not allow to take into account this term. Throughout the paper, parameters $\boldsymbol{\omega}$ and $\boldsymbol{\vartheta}$ do not depend on the spatial coordinate thus the theory does not contain any additional terms related to the noncommutativity of a momentum and a coordinate.

Nevertheless, we insist that the Hamiltonian formalism can be constructed but in the framework of non-Hermitian quantum mechanics. Moreover, the non-Hermitian Hamiltonian formalism allows the alternative explanation, which does not necessarily include many-particle effects as the possible mechanism of explanation. In order to introduce the Hamiltonian, we first construct the wave equation

$$G^{-1}(p_0, p_i)|\Psi\rangle = 0, \tag{5}$$

where for the spatially isotropic case, which contains all important physics, Green's function associated with action, Eq. (4) is given by

$$G^{-1}(p_0, p_i) = v_F\sigma^0 p_0 - v_F\sigma^i p_i - \omega^i p_i - \sigma^i\vartheta_i p_0. \tag{6}$$

Using the above expression, Eq. (5) can be easily rewritten in a conventional form, where the Hamiltonian in the left-hand side is the function of only three-dimensional momentum. After simple algebra, one arrives to the following two wave equations:

$$\mathcal{H}|\Psi^R\rangle = \varepsilon_R|\Psi^R\rangle, \quad \mathcal{H}^\dagger|\Psi^L\rangle = \varepsilon_L|\Psi^L\rangle, \tag{7}$$

where the non-Hermitian Hamiltonian takes form

$$\mathcal{H} = (i\Gamma + K)/(1-\beta^2), \quad \Gamma = \boldsymbol{\sigma}\cdot[\mathbf{p}\times\boldsymbol{\vartheta}],$$
$$K = [v_F\boldsymbol{\sigma} + \sigma_0(\boldsymbol{\omega}+\boldsymbol{\vartheta})]\cdot\mathbf{p} + (\boldsymbol{\sigma}\cdot\boldsymbol{\vartheta})(\boldsymbol{\omega}\cdot\mathbf{p})/v_F, \tag{8}$$

and $\beta = \vartheta/v_F$. This is the Hamiltonian of types III and IV non-Hermitian Weyl fermions and is our main result. This Hamiltonian can be also obtained directly from the action, Eq. (4), if one writes the wave equation as the Euler-Lagrange equation for the Dirac field. In Eq. (7), we have defined the R (right) and L (left) wave functions. It is worth mentioning that use of so called dual basis (R, L) is a convenient step for non-Hermitian systems, which allows to restore the common structure of Hilbert space [29–31].

Now one can easily obtain the spectrum of non-Hermitian and conjugated Hamiltonians from Eq. (7). The spectra are coincides with each other, namely,

$$\varepsilon = \varepsilon_R = \varepsilon_L^* = \frac{\mathcal{A}(\mathbf{p}) \pm \sqrt{\mathcal{B}(\mathbf{p})}}{1-\beta^2}, \quad \mathcal{A}(\mathbf{p}) = (\boldsymbol{\vartheta}+\boldsymbol{\omega})\cdot\mathbf{p},$$
$$\mathcal{B}(\mathbf{p}) = [(\boldsymbol{\vartheta}+\boldsymbol{\omega})\cdot\mathbf{p}]^2 + (1-\beta^2)\left[v_F^2p^2 - (\boldsymbol{\omega}\cdot\mathbf{p})^2\right], \tag{9}$$

where $p = |\mathbf{p}|$. Note that the Hamiltonian of form $\mathcal{H} = a\sigma_0 + (\mathbf{b} + i\mathbf{c})\boldsymbol{\sigma}$ has the spectrum $\varepsilon = a \pm \sqrt{\mathbf{b}^2 - \mathbf{c}^2 + 2i\mathbf{b}\cdot\mathbf{c}}$, which contains exceptional point due to term $\mathbf{b}\cdot\mathbf{c}$. In our case, $\mathbf{b}$ is proportional (collinear) to $\mathbf{p}$ and $\mathbf{c}$ is proportional to vector product $[\mathbf{p}\times\boldsymbol{\vartheta}]$, thus $\mathbf{b}\cdot\mathbf{c} = 0$ and the expression

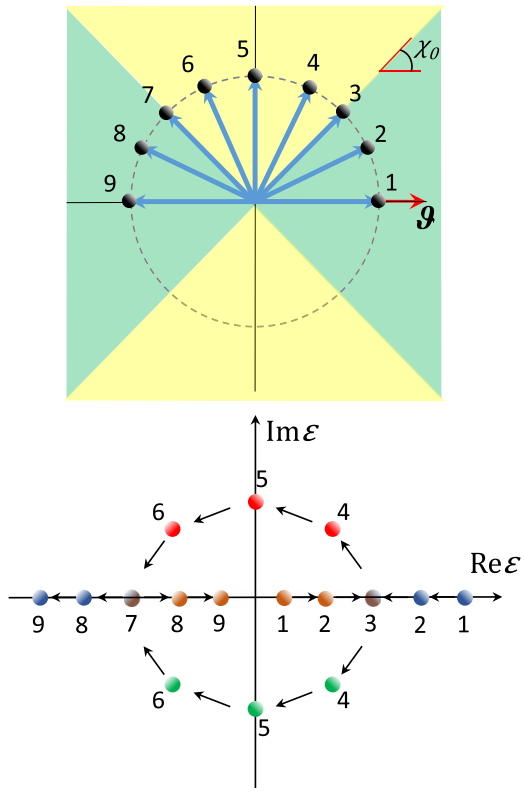

FIG. 1. (Top) It is shown the segments of angles between vectors $\boldsymbol{\vartheta}$ (red arrow) and $\mathbf{p}$ (blue arrow), where the imaginary part of spectrum, Im(ε) is zero (green) and nonzero (yellow). The angle $\chi_0 = \arcsin(1/\beta)$ corresponds to the direction of the momentum vector relative to vector $\boldsymbol{\vartheta}$, at which the transition from the real to complex spectrum occurs. The black dots represent different directions of the momentum relative to vector $\boldsymbol{\vartheta}$. (Bottom) It is shown the evolution (black arrows) of the real and imaginary parts of the spectrum Eq. (9) when the momentum direction changes from position 1 to position 9 (see the upper part of the figure). The brown and blue dots correspond to the hole and electronic states, respectively, while the red and green dots correspond to the complex spectrum with positive and negative imaginary parts, respectively. Dots 3 and 7 correspond to the transition points from the real to complex spectrum in Eq. (9) at vanishing $\mathcal{B}(\mathbf{p})$.

under the root always is real. For simplicity, we set $\boldsymbol{\omega} = 0$ for a further discussion. This does not affect the outcome, since the nonhermiticity is described by term $i\Gamma$. Then the Hamiltonian from Eq. (8) can be rewritten in the form

$$\mathcal{H} = [\boldsymbol{\sigma} \cdot (v_F \mathbf{e}_p + i\vartheta \sin\chi \mathbf{e}_\chi)p + \boldsymbol{\vartheta} \cdot \mathbf{p}]/(1-\beta^2), \qquad (10)$$

where the unit vector $\mathbf{e}_p$ is directed along the momentum $\mathbf{p}$ and the unit vector $\mathbf{e}_\chi$ is directed along the direction of the cross product $[\mathbf{p} \times \boldsymbol{\vartheta}]$. For values $\vartheta < v_F$ ($\beta < 1$), the parameter ϑ renormalizes the velocity $\partial\varepsilon/\partial \boldsymbol{p}$ due to coefficient $1/(1-\beta^2)$ and results in slope (tilt). For $\vartheta > v_F$ ($\beta > 1$), the spectrum in Eq. (9) is real in the segment $|\sin\chi| < \beta^{-1}$. In contrast, for $|\sin\chi| > \beta^{-1}$, the spectrum consists of complex-conjugated branches. Therefore we get the anisotropy with respect to spectrum's (Hamiltonian's) hermiticity (see Fig. 1). The eigenstates $|\Psi^R\rangle$ and $|\Psi^L\rangle$ are orthogonal: $\langle\Psi^L_\pm|\Psi^R_\mp\rangle = 0$ and $\langle\Psi^L_\pm|\Psi^R_\pm\rangle \neq 0$, where "$\pm$" corresponds to electron hole states in Eq. (9) (see Secs. A and B in Appendix for details). The existence of a segment with the real spectrum, despite the non-Hermitian nature of the Hamiltonian, is surprising. Nevertheless, we can prove the following statement. *If the non-Hermitian Hamiltonian $\mathcal{H}$ can be transform to Hermitian $\mathcal{H}_h$ one, using the similarity transformations with a nondegenerate matrix, then the eigenvalues of $\mathcal{H}$ are real.* Indeed, let us apply the similarity transformation, $S\mathcal{H}S^{-1}$ with the linear operator S in the from of nondegenerate matrix, $(S^{-1})^\dagger = (S^\dagger)^{-1}$, to Hamiltonian $\mathcal{H}$. Next, we assume that the following equality holds:

$$S\mathcal{H}S^{-1} = \mathcal{H}_h. \qquad (11)$$

Then $S\mathcal{H}S^{-1}|\Psi\rangle = \mathcal{H}_h|\Psi\rangle = \mathcal{E}|\Psi\rangle$, where $\mathcal{E}$ is real since Hamiltonian $\mathcal{H}_h$ is Hermitian. On the other hand due to linearity of operator S, this equation can be written as $\mathcal{H}|\overline{\Psi}\rangle = \mathcal{E}|\overline{\Psi}\rangle$, where $|\overline{\Psi}\rangle = S^{-1}|\Psi\rangle$. Thus the eigenvalues of the non-Hermitian Hamiltonian, which satisfies the condition (11), are real. Equation (11) can be rewritten in a new form

$$\mathcal{H}^\dagger = (S^\dagger S)\mathcal{H}(S^\dagger S)^{-1} = \eta\mathcal{H}\eta^{-1}, \qquad (12)$$

where we have introduced the Hermitian operator $\eta = S^\dagger S$. Equation (12) is the necessary and sufficient condition for the spectrum of Hamiltonain $\mathcal{H}$ to be real. If S is unitary matrix, then $S^\dagger S = 1$ and Eq. (12) recovers the hermicity of the Hamiltonian from Hermitian quantum mechanics. One can show that Hamiltonian (10) satisfies the condition (12) for $|\sin\chi| < \beta^{-1}$ segment (see Appendix C for details). For non-degenerate matrix $(S^{-1})^\dagger = (S^\dagger)^{-1}$, the condition in Eq. (12) coincides with the condition of pseudohermiticity [32–34]. This is the necessary condition for a spectrum to be real. The sufficient condition for the spectrum to be real is the existence of operator η in the form of $S^\dagger S$. The condition in Eq. (12) at $S^\dagger S = \eta$ is known as $\eta-$ hermiticity. We call Hamiltonains $\mathcal{H}$ and $\mathcal{H}_h$ from Eq. (11) equivalent, since they have the same real spectrum even if one of them is non-Hermitian. The equivalence of two Hamiltonians in that sense is the necessary and sufficient condition to have a real valued spectrum.

III. TOPOLOGICAL PROTECTION AND CHERN NUMBER

We continue to investigate the spectrum of Weyl fermions of types III and IV. It is worth mentioning, that Weyl points are topologically protected with respect to external perturbations. The spectrum remains gapless, for the case of unit matrix perturbation, $H \to H + IU_0$, which causes the shift of Weyl points with respect to energy and momentum, $\varepsilon \to \varepsilon(p - p_0) + \varepsilon(p_0)$, where p_0 satisfies to the condition $[(\boldsymbol{\vartheta} + \boldsymbol{\omega}) \cdot \mathbf{p}_0 + U_0]^2 + [1-\beta^2][v_F^2 p_0^2 - (\boldsymbol{\omega} \cdot \mathbf{p}_0 + U_0)^2] = 0$. Next, the perturbation in the form of a Pauli matrix, $H \to H + \boldsymbol{\sigma}\mathbf{U}$ results in the following spectrum:

$$\varepsilon = [\mathcal{E}_1(\mathbf{p}) \pm \mathcal{E}_2(\mathbf{p})]/(1-\beta^2), \qquad (13)$$

where $\mathcal{E}_1(\mathbf{p}) = \mathcal{A}(\mathbf{p}) + \boldsymbol{\vartheta} \cdot \mathbf{U}/v_F$ and $\mathcal{E}_2(\mathbf{p}) = \sqrt{\mathcal{E}_1^2(\mathbf{p}) + (1-\beta^2)\xi(\mathbf{p})}$, with $\xi(\mathbf{p}) = (v_F\mathbf{p} + \mathbf{U})^2 - (\boldsymbol{\omega} \cdot \mathbf{p})^2$ and $\mathcal{A}(\mathbf{p})$ is given in Eq. (9). This spectrum has a shift with respect to the initial one, Eq. (9), but does not contain a gap.

It is as well useful to investigate the stability of spectrum with the help of topological invariant-Chern number. For a non-Hermitian Hamiltonian, the Chern number can be written

as [31,36]

$$\mathcal{N} = \frac{1}{4\pi} \oint i\partial_{\mathbf{p}} \times \langle \Psi^L | \partial_{\mathbf{p}} | \Psi^R \rangle \cdot d\mathbf{S}, \tag{14}$$

where the integration is carried out over a closed surface enclosing the Weyl point (see Fig. 2). The Chern number defined in Eq. (14) must vanish, if the Hamiltonian has certain symmetries, namely, $\mathcal{H}(\mathbf{p}) = \mathcal{H}^T(\mathbf{p})$ (complex symmetric Hamiltonian which corresponds to C symmetry with $c = \sigma_0$ [35], where σ_0 is unit matrix), $\sigma_x \mathcal{H}(\mathbf{p}) \sigma_x = \mathcal{H}^T(\mathbf{p})$ (pseudo-Hermitian and real Hamiltonian which corresponds to C symmetry with $c = \sigma_x$ [35]) or $\mathcal{H}(\mathbf{p}) = \mathcal{H}^T(-\mathbf{p})$ (Hermitian-conjugate time reversal symmetry TRS†). The Hamiltonian does not satisfies any of these conditions, which indicates of topological protection of Chern invariant for the Hamiltonian under consideration. Next, the integration in Eq. (14) is performed with the help of Stoke's theorem in Appendix D. The result is an integer number, namely, $\mathcal{N}_\pm = \pm 1$. Thus one can see that the Chern number remains nonzero and integer despite the fact that the Hamiltonian is non-Hermitian. Apparently, this is a guarantee of the topological stability of the Weyl points of new types. Below we study the Landau levels and show that the zero Landau level, which is interpreted as a spectral flow, is purely real. This is another proof that the Chern number of Weyl points of types III and IV does not vanish despite presence of non-Hermiticity.

IV. LANDAU LEVELS AND SPECTRAL FLOW

Here we study the Landau levels for Weyl spectra of new types in presence of perpendicular magnetic field. The magnetic field breaks the T symmetry, which should lead to the opening of the band gap. However, in topologically nontrivial systems, so-called spectral fluxes arise in form of unidirectional chiral modes (see, for a review, Ref. [37]). We will verify that, despite the fact that our system is non-Hermitian, there are such spectral fluxes and they are purely real, which is an additional proof of the nontriviality of the nonzero Chern number. We consider the general case of nonzero $\boldsymbol{\omega} \neq 0$. In presence of a magnetic field $\mathbf{B} = (0, 0, B > 0)$, one has to shift the momentum $\mathbf{p} \to \mathbf{p} + e/c\mathbf{A}$ in Hamiltonian and $\nabla \times \mathbf{A} = \mathbf{B}$. Then, using the Landau gauge, we obtain the following equation for eigenvalues ε_n:

$$[\hat{\mathcal{M}} - \varepsilon + \omega_x p_x + \omega_z p_z] |\Psi\rangle = 0, \tag{15}$$

where the first term on the left-hand side consists of magnetic field

$$\hat{\mathcal{M}} = \upsilon_F \sigma_x \left(p_x + \frac{\varepsilon}{\upsilon_F^2} \vartheta_x - \frac{e}{c} By \right) + \upsilon_F \sigma_y \left(p_y + \frac{\varepsilon}{\upsilon_F^2} \vartheta_y \right) + \upsilon_F \sigma_z \left(p_z + \frac{\varepsilon}{\upsilon_F^2} \vartheta_z \right) - \omega_x \frac{e}{c} By. \tag{16}$$

For simplicity, further we set $\omega_y = 0$, and to solve the eigenvalues problem, we switch to a moving frame of reference using the Lorentz boost, $p_\nu = g_{\nu\mu} \tilde{p}_\mu$, with metric tensor

$$g_{\nu\mu} = \begin{pmatrix} \cosh\theta & \sinh\theta & 0 & 0 \\ \sinh\theta & \cosh\theta & 0 & 0 \\ 0 & 0 & 1 & 0 \\ 0 & 0 & 0 & 1 \end{pmatrix}, \tag{17}$$

where $\nu = t, x, y, z$ is a four-dimensional coordinate subscript and $\tanh\theta = \omega_x/\upsilon_F = \beta$. Thus we have

$$\Big[- e^{-\sigma_x \theta} \left(\hat{\tilde{p}}_t - \bar{p}_t \frac{\vartheta_x}{\upsilon_F} \sinh\theta \right) + \sigma_x e^{-\sigma_x \theta} \left(\hat{\tilde{p}}_x + \bar{p}_t \frac{\vartheta_x}{\upsilon_F} \cosh\theta - \frac{e}{c} By \right) + \sigma_y \left(\hat{\tilde{p}}_y - \bar{p}_t \frac{\vartheta_y}{\upsilon_F} \right) + \sigma_z \left(\hat{\tilde{p}}_z - \bar{p}_t \frac{\vartheta_z}{\upsilon_F} \right) \Big] |\Psi\rangle = 0. \tag{18}$$

For a stationary problem ($|\Psi\rangle \sim \exp i\varepsilon t$), after some algebra, we obtain Landau levels (further calculations are valid in the so-called magnetic regime, when $\beta < 1$. At $\beta \geqslant 1$ (electric regime), the electron energy is not quantized:

$$\varepsilon_n = \mathrm{sgn}(n) \sqrt{2\upsilon_\perp^2 \hbar^2 l_B^2 n + \upsilon_\parallel^2 p_z^2} + \tilde{\omega}_z p_z,$$
$$\varepsilon_0 = (\pm \upsilon_\parallel + \tilde{\omega}_z) p_z, \tag{19}$$

where $l_B = \sqrt{\hbar c/|e|B}$ is a magnetic length and the remaining parameters have the form

$$\upsilon_\perp = \frac{\upsilon_F \gamma^{3/2}}{\sqrt{\bar{\omega}^2 - \frac{\gamma^2 \vartheta_z^2}{\upsilon_F^2}}}, \quad \upsilon_\parallel = \upsilon_F \gamma \frac{\bar{\omega} + \frac{\omega_z \vartheta_z}{\upsilon_F^2}}{\bar{\omega}^2 - \frac{\gamma^2 \vartheta_z^2}{\upsilon_F^2}}, \tag{20}$$

$$\tilde{\omega}_z = \frac{\bar{\omega}\omega_z + \gamma^2 \vartheta_z}{\bar{\omega}^2 - \frac{\gamma^2 \vartheta_z^2}{\upsilon_F^2}}, \quad \bar{\omega} = 1 + \frac{\omega_x \vartheta_x}{\upsilon_F^2}, \quad \gamma = \sqrt{1 - \beta^2}. \tag{21}$$

As can be easily seen, the Landau levels are generally complex. However, the zero Landau level is purely real. This means that there is a real spectral flux between electronlike and holelike states. The presence of such a flow implicitly indicates a nonzero Chern number, which is the consequence of the index theorem (see Ref. [38]).

V. DISCUSSION

Let investigate the spectrum in phase transition point $\upsilon_F = \vartheta$. For simplicity, we assume that vectors $\boldsymbol{\vartheta}$, $\boldsymbol{\omega}$ are parallel to $\mathbf{p}$. Then one has $(\boldsymbol{\vartheta} + \boldsymbol{\omega}) \cdot \mathbf{p} = \pm(\vartheta + \omega)p$, where "$\pm$" correspond to positive and negative directions of momentum $\mathbf{p}$. Let be $\upsilon_F > \omega$. This corresponds to phase transition between types I and III. The electron states with positive momentum and hole states with negative momentum in phase transition point can be associated with infinite group velocity $\partial\varepsilon/\partial p$. Indeed, in this case, from Eq. (9), one has

$$\lim_{\vartheta \to \upsilon_F} \varepsilon \to \infty. \tag{22}$$

Such situation is described by vertical line. The second branch of spectrum originates from electron states with negative momentum and hole states with positive momentum. For these states, from Eq. (9), we have

$$\lim_{\vartheta \to \upsilon_F} \varepsilon = -\frac{\upsilon_F^2 p^2 - (\boldsymbol{\omega} \cdot \mathbf{p})^2}{2(\boldsymbol{\vartheta} + \boldsymbol{\omega}) \cdot \mathbf{p}}. \tag{23}$$

These two branches for the cases $\upsilon_F > \vartheta$, $\upsilon_F = \vartheta$ and $\upsilon_F < \vartheta$ are provided at Fig. 3 in case of type III (the qualitative picture for the case of type IV is similar). Let discuss these transitions in details. To do this, let consider the linear function $y = (a - b)x$. For $a > b$, this function describes the line

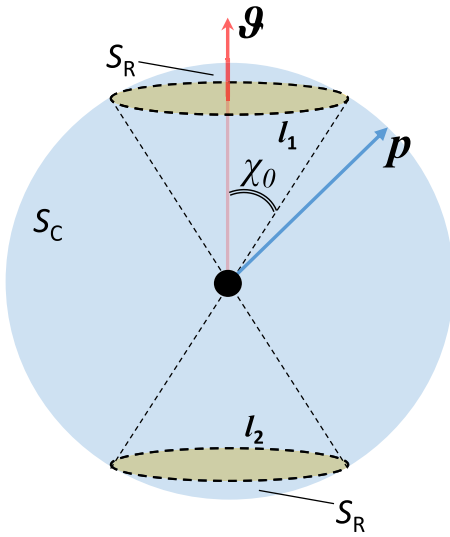

FIG. 2. It is shown a closed surface in momentum space enclosing the Weyl point. The surface is divided into two regions: the spectrum of Hamiltonian, Eq. (10), is real in the region S_{R} and complex in the region S_{C}. The lines $\boldsymbol{l}_1$ and $\boldsymbol{l}_2$ represent the boundaries between S_{R} and S_{C}. The vector $\boldsymbol{\vartheta}$ is directed along Z axis.

with positive slope. At point $a = b$, the continuous transition from positive to negative slope occurs. At the same time, point $a = b$ corresponds to horizontal line, i.e., the transition occurs through X axis. Is it possible to make a phase transition from positive slope to negative through Y axis? This transition correspond to type I-III (II-IV) and it is completely different compared to previous one. The main difference is that during the phase transition there is the swapping of the electron and hole states. Such a kind of transition can be described with the function of the form $y = x/(a - b)$. For $a > b$, this function describes the straight line with positive slope. For $a < b$, the slope is negative. Point $a = b$ corresponds to the transition from the positive to negative slope. However, compared to the previous example, $(a - b)x$, this is a singularity point. Thus the transition from the positive to negative slope is not continuous. In other words, in the second example, conditions $a > b$ and $a < b$ correspond to the fundamentally different phases, and the continuous transition between them is forbidden. Now, it becomes clear that types I and II are not topologically different since the continuous transition is allowed. Consequently, in this context, types I and III, I and IV are topologically different phases. Note that the discussion above is true only for one branch (in our case, it is the red line). For the blue branch, there is no inversion of the electron and hole parts of the spectrum. Indeed, the slope of the blue

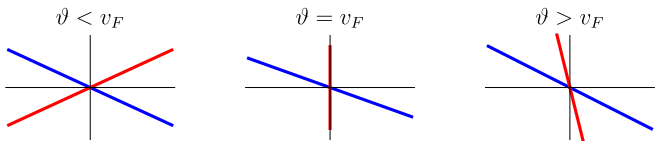

FIG. 3. The electron spectrums of types I (left) and III (right). The vertical axis is energy and the horizontal axis is momentum. The spectrum during the phase transition I-III (middle).

branch of the spectrum does not depend on the ratio between v_F and ϑ.

Finally, let us discuss the possible origin of the non-Hermitian Weyl Hamiltonian of types III and IV. The authors of Ref. [27] suggest to associate the Weyl fermions of types III and IV with many-particle effects. However, it can be provided the alternative interpretation as well. The alternative interpretation does not depend directly on the many-particle effects. We present the explanation in a general form, keeping in mind the two-band model of the band structure. The wave function in the two-band model has the form $|\Psi_{\mathbf{p}}\rangle = C_u|u_{\mathbf{p}}\rangle + C_v|v_{\mathbf{p}}\rangle$, where amplitude $C_{u/v}$ corresponds to $|u_{\mathbf{p}}\rangle/|u_{\mathbf{p}}\rangle$ Bloch's function. Multiplying the wave equation $H|\Psi_{\mathbf{p}}\rangle = E_{\mathbf{p}}|\Psi_{\mathbf{p}}\rangle$ by $\langle u_{\mathbf{p}}|$ and $\langle v_{\mathbf{p}}|$, we obtain the system of equations for the amplitudes

$$\begin{pmatrix} H^{\mathbf{p}}_{uu} & H^{\mathbf{p}}_{uv} \\ H^{\mathbf{p}}_{vu} & H^{\mathbf{p}}_{vv} \end{pmatrix} \begin{pmatrix} C_u \\ C_v \end{pmatrix} = E_{\mathbf{p}} \begin{pmatrix} S^{\mathbf{p}}_{uu} & S^{\mathbf{p}}_{uv} \\ S^{\mathbf{p}}_{vu} & S^{\mathbf{p}}_{vv} \end{pmatrix} \begin{pmatrix} C_u \\ C_v \end{pmatrix} = [f_0(\mathbf{p}) + \sigma_i f_i(\mathbf{p})](C_u \; C_v)^T, \quad (24)$$

where $H^{\mathbf{p}}_{ab} = \langle a_{\mathbf{p}}|H|b_{\mathbf{p}}\rangle$ is the matrix element of the Hamiltonian, with $a, b = u, v$, and $S^{\mathbf{p}}_{ab} = \langle a_{\mathbf{p}}|b_{\mathbf{p}}\rangle = \int a^*_{\mathbf{p}}(\mathbf{r}) b_{\mathbf{p}}(\mathbf{r}) d^3\mathbf{r}$ is the overlap integral. Typically, the Bloch functions are taken to be orthogonal, thus in Eq. (24), the overlap matrix becomes a unit matrix, $S^{\mathbf{p}}_{ab} = \delta_{ab}$. However, in real materials, this is not always true and the off-diagonal elements of the overlap matrix do not vanish (for instance, one of the reason is indeed many-particle effects) [39–44]. Let introduce the Bloch functions $u_{\mathbf{p}}(\mathbf{r}) = \sum_{\mathbf{R}} e^{-i\mathbf{p}(\mathbf{r}-\mathbf{R})}\phi_u(\mathbf{r} - \mathbf{R})$ and $v_{\mathbf{p}}(\mathbf{r}) = \sum_{\mathbf{R}} e^{-i\mathbf{p}(\mathbf{r}-\mathbf{R})}\phi_v(\mathbf{r} - \mathbf{R})$, where ϕ_u and ϕ_v are the atomic orbitals, corresponding to bands u and v, respectively, and $\mathbf{R}$ is a radius vector of a given atom at the lattice site. Then the off-diagonal overlap integral can be written as $\int u^*_{\mathbf{p}}(\mathbf{r}) v_{\mathbf{p}}(\mathbf{r}) d^3\mathbf{r} = \sum_{\mathbf{R}\mathbf{R}'} e^{i\mathbf{p}(\mathbf{R}-\mathbf{R}')} \int \phi^*_u(\mathbf{r} - \mathbf{R}')\phi_v(\mathbf{r} - \mathbf{R}) d^3\mathbf{r}$. Atomic orbitals corresponding to the same atom ($\mathbf{R} = \mathbf{R}'$) are orthogonal, $\int \phi^*_a(\mathbf{r} - \mathbf{R}')\phi_b(\mathbf{r} - \mathbf{R}) d^3\mathbf{r} = \delta_{ab}$. However, at different $\mathbf{R} \neq \mathbf{R}'$, generally speaking these orbitals are not orthogonal, which results in the nonzero off-diagonal elements of overlap matrix $S^{\mathbf{p}}_{ab}$. At the same time, we note that the Bloch functions at the Weyl point will be orthogonal, since at this point, the time reversal symmetry is not broken. This means that $\langle u_{\mathbf{p}_W}|\mathcal{T}u_{\mathbf{p}_W}\rangle = 0$, where $\mathcal{T}$ is the time reversal operator [17,18]. Since $\mathcal{T}|u_{\mathbf{p}_W}\rangle = |v_{\mathbf{p}_W}\rangle$ then $\langle u_{\mathbf{p}_W}|v_{\mathbf{p}_W}\rangle = 0$. Further, the Eq. (24) can be rewritten as $(S^{\mathbf{p}})^{-1}[f_0(\mathbf{p}) + \sigma_i f_i(\mathbf{p})](C_u \quad C_v)^T = \tilde{\mathcal{H}}(C_u \quad C_v)^T = \tilde{\varepsilon}(C_u \quad C_v)^T$, where $S^{\mathbf{p}}_{ab}$ is a matrix on the right-hand side of Eq. (24). In the vicinity of Weyl point, one has $f_i(\mathbf{p}) \approx v_F p_i$ and $f_0(\mathbf{p}) \approx \boldsymbol{\omega} \cdot \mathbf{p}$. If one requires that the overlap matrix in Pauli basis has components $S^{\mathbf{p}}_{uu(vv)} = 1 \mp \vartheta_z/v_F$, $S^{\mathbf{p}}_{uv} = (i\vartheta_y - \vartheta_x)/v_F = (S^{\mathbf{p}}_{vu})^*$, then the effective Hamiltonian, $\tilde{\mathcal{H}} = (S^{\mathbf{p}}_{ab})^{-1}[f_0(\mathbf{p}) + \sigma_i f_i(\mathbf{p})]$ completely coincides with the Hamiltonian from Eq. (8) with the same prefactor $1/(1 - \beta^2)$. Thus the origin of this Hamiltonian can be related with the overlap between Bloch functions. For 1D chain, such a Hamiltonian has been recently introduced by generalizing the Su-Schrieffer-Heeger model in the non-Hermitian case [45].

VI. CONCLUSION

To conclude, we have provided the theory of type III and IV Weyl semimetals within the non-Hermitian Hamiltonian formalism. The spectrum of this Weyl Hamiltonian exhibits an unusual type of anisotropy in momentum space, namely, for some directions, the spectrum is real, in contrast for other directions it is complex. The necessary and sufficient conditions for the spectrum to be real is provided. It is shown that the type III and IV Weyl points are topologically stable and the Chern number is equal to ± 1 despite to the fact that the Hamiltonian is not Hermitian. Apart from that, we have demonstrated that the zero Landau level is real, which means that there is a real spectral flow between electronlike and holelike states. The formal analogy with the index theorem indicates the presence of a nonzero Chern number as well. Additionally, we speculated on the possible origin of the non-Hermitian Hamiltonian.

ACKNOWLEDGMENTS

We are grateful to G. E. Volovik, J. Nissinen, and T. L. Schmidt for fruitful discussions. Z.A. acknowledges support from the Russian Science Foundation Grant No. 22-72-00110.

APPENDIX A: THE ORTHOGONALITY CONDITIONS

We write the spectrum from Eq. (9) in the main text with additional subscripts as

$$\varepsilon_{R,\pm} = \varepsilon^*_{L,\pm} = \frac{\mathcal{A}(\mathbf{p}) \pm \sqrt{\mathcal{B}(\mathbf{p})}}{1-\beta^2}, \tag{A1}$$

where "$\pm$" are associated with electron and hole states. The corresponding eigenvectors are denoted by $|\Psi^{R,L}_{\pm}\rangle$, which satisfy wave equations $\mathcal{H}|\Psi^R_{\pm}\rangle = \varepsilon_{R,\pm}|\Psi^R_{\pm}\rangle$, and $\mathcal{H}^\dagger|\Psi^L_{\pm}\rangle = \varepsilon^*_{L,\pm}|\Psi^L_{\pm}\rangle$. In phases III and IV, the spectrum is anysotropic [see Eq. (9) from main text] with respect to space orientation of momentum vector: for some directions, the spectrum is real, in contrast, for other directions, it is complex. It is worth mentioning that for the real spectrum sector $\varepsilon_R = \varepsilon_L = \varepsilon$, where "$\pm$" is omitted. The existence of domain, where $\mathrm{Im}(\varepsilon) \neq 0$ is the main distinguishing feature of the new phases, III and IV. Apart from this, in domain of complex spectrum $\varepsilon^*_{\pm} = \varepsilon_{\mp}$, which leads to important consequences. The main one is related with scalar product $\langle\Psi^L_\alpha|\Psi^R_\beta\rangle$. Let consider the following 2×2 matrix:

$$\begin{pmatrix} \langle\Psi^L_+|\mathcal{H}|\Psi^R_+\rangle & \langle\Psi^L_+|\mathcal{H}|\Psi^R_-\rangle \\ \langle\Psi^L_-|\mathcal{H}|\Psi^R_+\rangle & \langle\Psi^L_-|\mathcal{H}|\Psi^R_-\rangle \end{pmatrix}. \tag{A2}$$

Applying the Hamiltonian inside matrix elements on the right- and left-hand sides, one obtains

$$\begin{pmatrix} \varepsilon_+\langle\Psi^L_+|\Psi^R_+\rangle & \varepsilon_-\langle\Psi^L_+|\Psi^R_-\rangle \\ \varepsilon_+\langle\Psi^L_-|\Psi^R_+\rangle & \varepsilon_-\langle\Psi^L_-|\Psi^R_-\rangle \end{pmatrix} = \begin{pmatrix} \varepsilon_+\langle\Psi^L_+|\Psi^R_+\rangle & \varepsilon_+\langle\Psi^L_+|\Psi^R_-\rangle \\ \varepsilon_-\langle\Psi^L_-|\Psi^R_+\rangle & \varepsilon_-\langle\Psi^L_-|\Psi^R_-\rangle \end{pmatrix}. \tag{A3}$$

From the above equation, it is obvious that $\langle\Psi^L_\pm|\Psi^R_\mp\rangle = 0$ and $\langle\Psi^L_\pm|\Psi^R_\pm\rangle \neq 0$.

APPENDIX B: THE FORM OF EIGENSTATES

The Hamiltonian under consideration has the form

$$\mathcal{H} = A(\mathbf{p})\sigma_0 + [\boldsymbol{D}(\mathbf{p}) + i\boldsymbol{C}(\mathbf{p})]\cdot\boldsymbol{\sigma}, \tag{B1}$$

where $\boldsymbol{D}\cdot\boldsymbol{C} = 0$. The spectrum of this Hamiltonian is given by

$$\varepsilon_{R,\pm} = \varepsilon^*_{L,\pm} = \varepsilon_\pm = A \pm \sqrt{D^2 - C^2}, \tag{B2}$$

where $C = |\boldsymbol{C}|$ and $D = |\boldsymbol{D}|$. Particularly, for the case under consideration in main text, the parameters are $A = (\boldsymbol{\omega}\cdot\mathbf{p} + \boldsymbol{\vartheta}\cdot\mathbf{p})/(1-\beta^2)$, $\boldsymbol{D} = (\upsilon_F\mathbf{p} + \frac{1}{\upsilon_F}\boldsymbol{\vartheta}(\boldsymbol{\omega}\cdot\mathbf{p}))/(1-\beta^2)$ and $\boldsymbol{C} = [\mathbf{p}\times\boldsymbol{\vartheta}]/(1-\beta^2)$. The eigenstates of the Hamiltonian are given by

$$|\Psi^R_\pm\rangle = N_\pm\begin{pmatrix} C_z - iD_z \mp i\sqrt{D^2-C^2} \\ C_x + i(C_y - D_x) + D_y \end{pmatrix},$$
$$|\Psi^L_\pm\rangle = N_\pm\begin{pmatrix} C_z + iD_z \pm i(\sqrt{D^2-C^2})^* \\ C_x + i(C_y + D_x) - D_y \end{pmatrix}, \tag{B3}$$

where "$*$" means the complex conjugation. Using the form of eigenstates in Eq. (B3), one can show that $\langle\Psi^L_\pm|\Psi^R_\mp\rangle = 0$. Further, the direct calculations give $\langle\Psi^L_\pm|\Psi^R_\pm\rangle = -2(D^2-C^2) \mp 2i(C_z - iD_z)\sqrt{D^2-C^2}$. Therefore the normalizing factor $N_\pm$ of the eigenfunctions is equal to

$$N_\pm = \frac{1}{i\sqrt{2(D^2-C^2) \pm 2i(C_z - iD_z)\sqrt{D^2-C^2}}}. \tag{B4}$$

Let us explore the topology of the eigenstates obtained above. Without loss of generality, we consider the simplest case when $\boldsymbol{\omega} = 0$ and $\boldsymbol{\vartheta} = (0, 0, \vartheta)$. We write the eigenfunctions in spherical coordinates

$$|\Psi^R_\pm\rangle = \frac{\exp(-i\chi)}{\sqrt{2\sqrt{1-\beta^2\sin^2\theta}(\sqrt{1-\beta^2\sin^2\theta} \pm \cos\theta)}} \times \begin{pmatrix} (\cos\theta \pm \sqrt{1-\beta^2\sin^2\theta}) \\ (1+\beta)\sin\theta e^{i\varphi} \end{pmatrix}, \tag{B5}$$

$$|\Psi^L_\pm\rangle = \frac{\exp(-i\chi)}{\sqrt{2\sqrt{1-\beta^2\sin^2\theta}(\sqrt{1-\beta^2\sin^2\theta} \pm \cos\theta)}} \times \begin{pmatrix} (\cos\theta \pm \sqrt{1-\beta^2\sin^2\theta}) \\ (1-\beta)\sin\theta e^{i\varphi} \end{pmatrix}, \tag{B6}$$

where χ is some arbitrary phase. However, these eigenfunctions contain points where the uniqueness is lost. The existence of such points is the source of nontrivial topology. In our case, these points correspond to angles $\theta = 0$ and $\theta = \pi$, which exactly coincides with the Hermitian Hamiltonian in the form of a monopole. At point $\theta = 0$, the eigenfunction has the form (for concreteness, we consider only $\Psi^{R,L}_+$)

$$|\Psi^{R,L}_+((\theta = 0)\rangle = \exp(-i\chi)\begin{pmatrix} 1 \\ 0 \end{pmatrix}. \tag{B7}$$

Therefore, for uniqueness of the above function, it is necessary to set $\chi = 0$ (northern gauge). However, this gauge is not suitable for point $\theta = \pi$. Indeed, at this point, the eigenfunctions have the form

$$|\Psi^{R,L}_+(\theta = \pi)\rangle = \exp(-i\chi)\begin{pmatrix} 0 \\ \sqrt{\frac{1\pm\beta}{1-\beta}}e^{i\phi} \end{pmatrix}. \tag{B8}$$

We see that for the uniqueness of this function, it is necessary to set $\chi = \phi$ (southern gauge). Thus the multivaluedness of

the eigenstates cannot be eliminated by a global gauge choice in form of smooth function. Different gauge phases must be used in the northern and southern hemispheres. Thus, consequently for the eigenfunctions of the southern hemisphere, we have

$$\left|\overset{\mathrm{S}}{\Psi^R}_{+}\right\rangle = \frac{1}{\sqrt{2\sqrt{1-\beta^2\sin^2\theta}(\sqrt{1-\beta^2\sin^2\theta}\pm\cos\theta)}} \times \begin{pmatrix}(\cos\theta\pm\sqrt{1-\beta^2\sin^2\theta})e^{-i\varphi}\\(1+\beta)\sin\theta\end{pmatrix}, \tag{B9}$$

$$\left|\overset{\mathrm{S}}{\Psi^L}_{+}\right\rangle = \frac{1}{\sqrt{2\sqrt{1-\beta^2\sin^2\theta}(\sqrt{1-\beta^2\sin^2\theta}\pm\cos\theta)}} \times \begin{pmatrix}(\cos\theta\pm\sqrt{1-\beta^2\sin^2\theta})e^{-i\varphi}\\(1-\beta)\sin\theta\end{pmatrix}. \tag{B10}$$

And for the eigenfunctions of the northern hemisphere, we have

$$\left|\overset{\mathrm{N}}{\Psi^R}_{\pm}\right\rangle = \frac{1}{\sqrt{2\sqrt{1-\beta^2\sin^2\theta}(\sqrt{1-\beta^2\sin^2\theta}\pm\cos\theta)}} \times \begin{pmatrix}(\cos\theta\pm\sqrt{1-\beta^2\sin^2\theta})\\(1+\beta)\sin\theta e^{i\varphi}\end{pmatrix}, \tag{B11}$$

$$\left|\overset{\mathrm{N}}{\Psi^L}_{\pm}\right\rangle = \frac{1}{\sqrt{2\sqrt{1-\beta^2\sin^2\theta}(\sqrt{1-\beta^2\sin^2\theta}\pm\cos\theta)}} \times \begin{pmatrix}(\cos\theta\pm\sqrt{1-\beta^2\sin^2\theta})\\(1-\beta)\sin\theta e^{i\varphi}\end{pmatrix}. \tag{B12}$$

We use these eigenstates in Appendix D for calculating of the Chern number.

APPENDIX C: REAL SPECTRUM OF PSEUDO-HERMITIAN HAMILTONIAN

From the main text, Eq. (12), it is clear, that $[\eta,\mathcal{H}] = \eta\mathcal{H}-\mathcal{H}\eta\neq 0$, for non-Hermitian $\mathcal{H}$. Indeed, otherwise $[\eta,\mathcal{H}]=0$ and one arrives to contradiction, namely, the conjugated Hamiltonian $\mathcal{H}^\dagger=\eta\mathcal{H}\eta^{-1}=\mathcal{H}\eta\eta^{-1}=\mathcal{H}$ is Hermitian. As an example, let consider the simple non-Hermitian matrix $M=\left(\begin{smallmatrix}1 & 1+\lambda\\ 1-\lambda & -1\end{smallmatrix}\right)$, where λ is the arbitrary number. Next, let find the matrix η, which satisfies the condition $M^\dagger=\eta M\eta^{-1}$. One can show that the η has the following form $\eta=\left(\begin{smallmatrix}\frac{r+q}{1+\lambda} & q\\ q & \frac{r-q}{1-\lambda}\end{smallmatrix}\right)$, where p, q are arbitrary numbers as well. Further, in order to have the real eigenvalues for matrix M, there must be possibility to present $\eta=S^\dagger S$. From these condition, one consequently obtains that $q, r\in\mathbb{R}$ and $\eta^\dagger=\eta$. Further, it is obvious, that the condition $\det(SS^\dagger)>0$ must be satisfied. This condition set limits on the choice of elements of matrix η. In our case, this condition brings us to inequality for p, q and λ, namely, $\frac{q^2-r^2}{\lambda^2-1}-q^2>0$. This inequality does not work for $\lambda^2>2$. Thus the eigenvalues of matrix M are real for $\lambda^2<2$.

Let now investigate our Hamiltonian in the same manner as the example above. For simplicity, we consider the case of $\boldsymbol{\vartheta}=(0,0,\vartheta)$. In this case, the Hamiltonian in Eq. (10) from main text is written as

$$\mathcal{H}=\frac{v_F}{1-\beta^2}\left[\begin{pmatrix}p_z & (1-\beta)(p_x-ip_y)\\ (1+\beta)(p_x+ip_y) & -p_z\end{pmatrix} + \beta p_z\sigma_0\right], \tag{C1}$$

where $\beta=\vartheta/v_F$ and σ_0 is the identity matrix. The matrix η has the form $\eta=\left(\begin{smallmatrix}a & b\\ b^* & d\end{smallmatrix}\right)$, where $a=\frac{r+bp_z}{(1-\beta)(p_x-ip_y)}$ and $d=\frac{r-bp_z}{(1+\beta)(p_x-ip_y)}$, $r,b\in\mathbb{C}$. From condition $\eta=S^\dagger S$, one gets that $q,r>0\in\mathbb{R}$ and the condition $\det(S^\dagger S)>0$ results in inequality for other parameters, $ad-|b|^2>0\in\mathbb{R}$. Using these conditions at $\beta<1$, one can show that matrix $\eta=S^\dagger S$ exists always. For example, $\eta=\left(\begin{smallmatrix}\frac{q}{1-\beta} & 0\\ 0 & \frac{q}{1+\beta}\end{smallmatrix}\right)$, where $q>0\in\mathbb{R}$. For $\beta>1$, the matrix $\eta=S^\dagger S$ exists only for $\frac{p_z^2}{p_x^2+p_y^2}<\beta^2-1$, which turns out to be $|\sin\chi|<\beta^{-1}$ in spherical coordinates, and this condition coincides with the one we have provided in Eq. (9) from main text. In this case the matrix has the form $\eta=\left(\begin{smallmatrix}\frac{p_z}{\beta-1} & -p_x+ip_y\\ -p_x-ip_y & \frac{p_z}{\beta+1}\end{smallmatrix}\right)$. In other words, for $|\sin\chi|<\beta^{-1}$ the Hamiltonian above, Eq. (C1) can be brought to Hermitian Hamiltonian using similarity transformations. namely, $S^{-1}\mathcal{H}S$ is the Hermitian operator, despite the fact that $\mathcal{H}$ is non-Hermitian. Additionally, it is worth pointing out, that redefinition of scalar product in Hilbert space (unitary theorem) in the following form $\langle\langle\Psi|\Psi\rangle\rangle_S\equiv\langle\Psi|S^\dagger S|\Psi\rangle$ does depend on time, if Hamiltonian satisfies the condition (12) from main text. Thus this means that the probability density does not depend on time, and the unitary condition is suited.

As one can observe from Eq. (12) from main text, in general the realness of spectrum is defined not only by the properties of operator by itself, but as well it influences on Hilbert space. It worth mentioning, that the $\mathcal{PT}$ symmetry for non-Hermitian quantum systems introduced by Bender [46], says that $\mathcal{PT}$ operator and Hamiltonian have the same eigenvectors. In this case Hamiltonian has the real spectrum, despite the fact that it is non-Hermitian. This requirements is the particular case of Eq. (12) from main text. Namely, to show this, let change a bit the matrix we have considered above, $M\Rightarrow\left(\begin{smallmatrix}1 & \lambda-1\\ \lambda+1 & -1\end{smallmatrix}\right)$. This matrix is not Hermitian and it does not have $\mathcal{PT}$ symmetry. However, the eigenvalues of this matrix are real for any real λ. This is related with the fact that matrix $\left(\begin{smallmatrix}1 & \lambda-1\\ \lambda+1 & -1\end{smallmatrix}\right)$ is equivalent to Hermitian matrix $\left(\begin{smallmatrix}0 & \lambda\\ \lambda & 0\end{smallmatrix}\right)$. Namely, there always exists the similarity transformation R, therefore, $R\left(\begin{smallmatrix}0 & \lambda\\ \lambda & 0\end{smallmatrix}\right)R^{-1}=\left(\begin{smallmatrix}1 & \lambda-1\\ \lambda+1 & -1\end{smallmatrix}\right)$.

APPENDIX D: CALCULATION OF CHERN NUMBER

The Chern number is given by the surface integral

$$\mathcal{N}_\alpha=\frac{1}{2\pi}\int_S\mathcal{F}^\alpha, \tag{D1}$$

where $\mathcal{F}^\alpha=-i\mathrm{tr}(P^\alpha\mathrm{d}P^\alpha\wedge\mathrm{d}P^\alpha)$ is the Berry curvature of α band, $\alpha=\pm$ and $\wedge$ denotes wedge product. Operator $P^\alpha=|\Psi^R_\alpha\rangle\langle\Psi^L_\alpha|$ is the spectral projector on the α band and the integration is carried out with respect to closed surface, enclosing

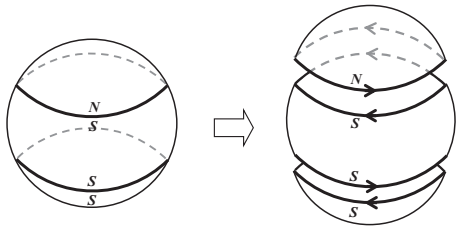

FIG. 4. Gauge on the integration sphere (left) and division of the sphere into three regions along the exceptional lines (right).

the Weyl point. Equation (D1) is completely equivalent to Eq. (14) from main text. We spit Eq. (D1) into two parts

$$\mathcal{N}_\alpha = \frac{1}{2\pi}\left(\int_{S_C} \mathcal{F}^\alpha + \int_{S_R} \mathcal{F}^\alpha\right), \tag{D2}$$

where surface domains S_C and S_R correspond to complex and real spectra (see Fig. 4). The region of the real spectrum consists of northern (N) and southern parts (S): $S_R = \overset{N}{S}_R + \overset{S}{S}_R$. Therefore the integral includes three terms

$$\mathcal{N}_\alpha = \frac{1}{2\pi}\left(\int_{S_C} \mathcal{F}^\alpha + \int_{\overset{N}{S}_R} \mathcal{F}^\alpha + \int_{\overset{S}{S}_R} \mathcal{F}^\alpha\right). \tag{D3}$$

Next, we use Stoke's theorem to go from integration of Berry curvature to integration of Berry connection. However, before doing this, it is necessary to correctly select the gauge of the eigenfunctions for the north and south poles. This gauge is important for regions $\overset{N}{S}_R$ and $\overset{S}{S}_R$, at the same time for region S_C, we can choose any gauge. To use the Stokes theorem, we break the sphere along the exceptional lines, as shown in Fig. 4 (left). According to Stoke's theorem the Chern number is defined as follows:

$$\int_S \mathcal{F} = \int_{\partial S} \mathcal{A}, \tag{D4}$$

where ∂S is the boundary of S and $\mathcal{A}$ is Berry connection. In our case $\partial S = \boldsymbol{l}_{1,2}$ (see Fig. 2). In spherical coordinates, for the Berry connection along the exceptional lines, we have

$$\mathcal{A}^{\pm}_{1,2} = i\langle\Psi^L_\pm|\mathrm{d}|\Psi^R_\pm\rangle_{\theta\to\chi_0,\pi-\chi_0} = i\langle\Psi^L_\pm|\partial_\varphi|\Psi^R_\pm\rangle_{\theta\to\chi_0,\pi-\chi_0} d\varphi \tag{D5}$$

where $\theta = \chi_0$ corresponds to exceptional line $\boldsymbol{l}_1$ and $\theta = \pi - \chi_0$ corresponds to exceptional line $\boldsymbol{l}_2$. Now, splitting the sphere as shown in Fig. 4 (right), we have

$$\begin{aligned}\mathcal{N}_\pm &= \frac{1}{2\pi}\left[\int_{l_1}\mathcal{A}_N - \int_{l_1}\mathcal{A}_S\right]_{\theta=\chi_0} + \frac{1}{2\pi}\left[\int_{l_2}\mathcal{A}_S - \int_{l_2}\mathcal{A}_S\right]_{\theta=\pi-\chi_0}\\ &= \int_0^{2\pi}\frac{d\varphi}{2\pi}\left[i\left\langle\overset{N}{\Psi^L}_\pm\middle|\partial_\varphi\middle|\overset{N}{\Psi^R}_\pm\right\rangle - i\left\langle\overset{S}{\Psi^L}_\pm\middle|\partial_\varphi\middle|\overset{S}{\Psi^R}_\pm\right\rangle\right]_{\theta=\chi_0}\\ &= \pm\int_0^{2\pi}\frac{d\varphi}{2\pi} = \pm 1.\end{aligned} \tag{D6}$$

Thus the Chern number remains nonzero and integer despite the fact that the Hamiltonian is non-Hermitian.

[1] A. Bansil, H. Lin, and T. Das, Rev. Mod. Phys. **88**, 021004 (2016).
[2] M. J. Gilbert, Commun. Phys. **4**, 70 (2021).
[3] Z. K. Liu, B. Zhou, Y. Zhang, Z. J. Wang, H. M. Weng, D. Prabhakaran, S.-K. Mo, Z. X. Shen, Z. Fang, X. Dai, Z. Hussain, and Y. L. Chen, Science **343**, 864 (2014).
[4] S. Borisenko, Q. Gibson, D. Evtushinsky, V. Zabolotnyy, B. Büchner, and R. J. Cava, Phys. Rev. Lett. **113**, 027603 (2014).
[5] B-J. Yang and N. Nagaosa, Nat. Commun. **5**, 4898 (2014).
[6] S.-Y. Xu, C. Liu, S. K. Kushwaha, R. Sankar, J. W. Krizan, I. Belopolski, M. Neupane, G. Bian, N. Alidoust, T.-R. Chang, H.-T. Jeng, C.-Y. Huang, W.-F. Tsai, H. Lin, P. P. Shibayev, F.-C. Chou, R. J. Cava, and M. Z. Hasan, Science **347**, 294 (2015).
[7] O. Vafek and A. Vishwanath, Annu. Rev. Condens. Matter Phys. **5**, 83 (2014).
[8] H. Weng, C. Fang, Z. Fang, B. A. Bernevig, and X. Dai, Phys. Rev. X **5**, 011029 (2015).
[9] S.-M. Huang, S.-Y. Xu, I. Belopolski, C.-C. Lee, G. Chang, B. Wang, N. Alidoust, G. Bian, M. Neupane, C. Zhang, S. Jia, A. Bansil, H. Lin, and M. Z. Hasan, Nat. Commun. **6**, 7373 (2015).
[10] S.-Y. Xu, I. Belopolski, N. Alidoust, M. Neupane, G. Bian, C. Zhang, R. Sankar, G. Chang, Z. Yuan, C.-C. Lee, S.-M. Huang, H. Zheng, J. Ma, D. S. Sanchez, BaoKai Wang, A. Bansil, F. Chou, P. P. Shibayev, H. Lin, S. Jia, and M. Z. Hasan, Science **349**, 613 (2015).
[11] B. Q. Lv, H. M. Weng, B. B. Fu, X. P. Wang, H. Miao, J. Ma, P. Richard, X. C. Huang, L. X. Zhao, G. F. Chen, Z. Fang, X. Dai, T. Qian, and H. Ding, Phys. Rev. X **5**, 031013 (2015).
[12] B. Bradlyn, J. Cano, Z. Wang, M. G. Vergniory, C. Felser, R. J. Cava, and B. A. Bernevig, Science **353**, aaf5037 (2016).
[13] T. Bzdušek, Q. Wu, A. Rüegg, M. Sigrist, and A. A. Soluyanov, Nature **538**, 75 (2016).
[14] R. Yu, H. Weng, Z. Fang, X. Dai, and X. Hu, Phys. Rev. Lett. **115**, 036807 (2015).
[15] G. Bian, T.-R. Chang, R. Sankar, S.-Y. Xu, H. Zheng, T. Neupert, C.-K. Chiu, S.-M. Huang, G. Chang, I. Belopolski, D. S. Sanchez, M. Neupane, N. Alidoust, C. Liu, BaoKai Wang, C.-C. Lee, H.-T. Jeng, C. Zhang, Z. Yuan, S. Jia, A. Bansil *et al.*, Nat. Commun. **7**, 10556 (2016).
[16] G. E. Volovik, *The Universe in a Helium Droplet* (Claverdon Press, Oxford, 2003).
[17] C. Herring, Phys. Rev. **52**, 361 (1937).
[18] C. Herring, Phys. Rev. **52**, 365 (1937).
[19] N. P. Armitage, E. J. Mele, and A. Vishwanath, Rev. Mod. Phys. **90**, 015001 (2018).
[20] G. E. Volovik and M. A. Zubkov, Nucl. Phys. B **881**, 514 (2014).
[21] A. A. Soluyanov, D. Gresch, Z. Wang, QuanSheng Wu, M. Troyer, X. Dai, and B. A. Bernevig, Nature (London) **527**, 495 (2015).
[22] Y. Sun, S.-C. Wu, M. N. Ali, C. Felser, and B. Yan, Phys. Rev. B **92**, 161107 (2015).

[23] Z. Wang, D. Gresch, A. A. Soluyanov, W. Xie, S. Kushwaha, X. Dai, M. Troyer, R. J. Cava, and B. A. Bernevig, Phys. Rev. Lett. **117**, 056805 (2016).
[24] I. Belopolski, D. S. Sanchez, Y. Ishida, X. Pan, P. Yu, S.-Y. Xu, G. Chang, T.-R. Chang, H. Zheng, N. Alidoust, G. Bian, M. Neupane, S.-M. Huang, C.-C. Lee, Y. Song, H. Bu, G. Wang, S. Li, G. Eda, H.-T. Jeng *et al.*, Nat. Commun. **7**, 13643 (2016).
[25] Y. Kedem, E. J. Bergholtz, and F. Wilczek, Phys. Rev. Res. **2**, 043285 (2020).
[26] C. De Beule and S. Groenendijk, T. Meng, and T. L. Schmidt, SciPost Phys. **11**, 095 (2021).
[27] J. Nissinen and G. E. Volovik, JETP Lett. **105**, 447 (2017).
[28] J. Nissinen and G. E. Volovik, J. Exp. Theor. Phys. **127**, 948 (2018).
[29] D. C. Brody, J. Phys. A: Math. Theor. **47**, 035305 (2014).
[30] E. J. Bergholtz, J. C. Budich, and F. K. Kunst, Rev. Mod. Phys. **93**, 015005 (2021).
[31] A. Ghatak and T. Das, J. Phys.: Condens. Matter **31**, 263001 (2019).
[32] A. Mostafazadeh, J. Math. Phys. **43**, 205214 (2002).
[33] A. Mostafazadeh, J. Math. Phys. **43**, 2814 (2002).
[34] A. Mostafazadeh, J. Math. Phys. **43**, 3944 (2002).
[35] K. Kawabata, K. Shiozaki, M. Ueda, and M. Sato, Phys. Rev. X **9**, 041015 (2019).
[36] H. Shen, B. Zhen, and L. Fu, Phys. Rev. Lett. **120**, 146402 (2018).
[37] P. Delplace, SciPost Phys. Lect. Notes, page 39, 2022
[38] M. F. Atiyah, V. K. Patodi, and I. M. Singer, Math. Proc. Cambridge Philos. Soc. **79**, 71 (1976).
[39] E. Antoncík and P. T. Landsberg, Proc. Phys. Soc. **82**, 337 (1963).
[40] V. Halpern, J. Phys. Chem. Solids **24**, 1495 (1963).
[41] N. Bernstein, M. J. Mehl, and D. A. Papaconstantopoulos, Phys. Rev. B **66**, 075212 (2002).
[42] W. A. Harrison and S. Ciraci, Phys. Rev. B **10**, 1516 (1974).
[43] J. Tejeda and N. J. Shevchik, Phys. Rev. B **13**, 2548 (1976).
[44] T. B. Boykin, P. Sarangapani, and G. Klimeck, J. Appl. Phys. **125**, 144302 (2019).
[45] T. B. Smith and A. Principi, Phys. E **126**, 114423 (2021).
[46] C. M. Bender, *PT Symmetry In Quantum and Classical Physics* (World Scientific, Singapore, 2019).